

# CHAPTER 131

## STATIC AND DYNAMIC LOADING TESTS ON THE HARO ARMOUR UNIT

L. Van Damme<sup>1</sup>

J. De Rouck<sup>2</sup>

L. Taerwe<sup>3</sup>

R. Dedeyne<sup>4</sup>

J. Degrieck<sup>5</sup>

### **1. ABSTRACT**

During the harbour extension works at Zeebrugge a new armour unit has been developed : the HARO. Tests in wave flume and wave tank showed a very good hydraulic stability, comparable to that of the dolos. Static and dynamic loading tests in the laboratory and pendulum tests on site confirm the HARO's excellent structural performance, comparable to that of the cube. Based on the results of exhaustive investigations one can state that the HARO is a safe and economical solution for the protection of maritime structures.

### **2. INTRODUCTION**

The HARO is a plain concrete block for the protection of maritime structures (breakwaters, sea walls, groynes ...) against wave attack. It found an extensive application in the harbour extension works at Zeebrugge. It is also currently being used for the Gwadar Port in Pakistan. The name HARO is registered by HAECON N.V.

The HARO is a compact concrete block with a large central opening (fig. 1). Both short sides are made wider at the base. The corners are asymmetrically tapered in plan. Thanks to the large central opening, the protuberances at the short sides and

-----  
<sup>1</sup>Ministry of Public Works, Coastal Department, Ostend, Belgium

<sup>2</sup>HAECON N.V. and Ghent State University, Ghent, Belgium

<sup>3</sup>Magnel Laboratory for Reinforced Concrete, Ghent State University, Ghent, Belgium

<sup>4</sup>Bureau SECO, Brussels, Belgium

<sup>5</sup>Department for Mechanics of Materials and Structures, Ghent State University, Ghent, Belgium.

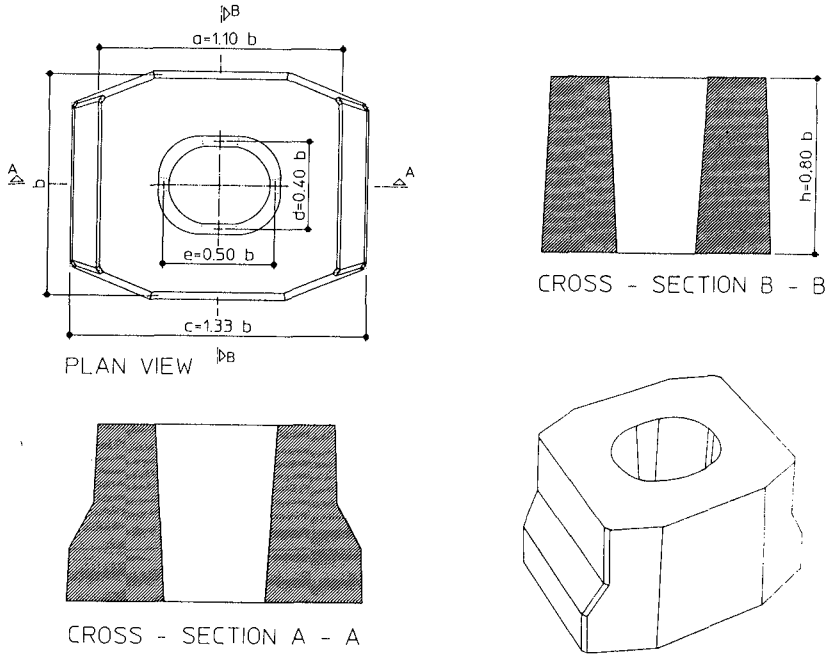


Figure 1. Geometry of the HARO armour unit

conform an appropriate placement pattern, a porosity as high as 51-53 % can be achieved.

An exhaustive laboratory investigation conducted at the Hydraulic Research Laboratory in Borgerhout (Antwerp) showed a very good hydraulic stability which is comparable to that of the dolos (De Rouck et al., 1987; Wens et al., 1990). However, the reliability of the armour layer and thus the whole rubble mound breakwater, not only depends on the hydraulic stability of the armour units but also to a large extent on their structural strength. Unfortunately, failures in the late seventies and in the early eighties showed this point all too clearly. In order to verify the structural strength of the HARO, static and dynamic loading tests were carried out in the Magnel Laboratory of Ghent State University and on the site.

### 3. STATIC LOADING TEST

The test set-up for the static loading test on a 150 kN HARO is shown in fig. 2. The block was turned on its side and placed on two supporting concrete beams with variable depth. On the upper surface, a circular steel disc (300 mm  $\varnothing$ ), on which the load  $P$  was applied, was placed. This load application point is located on the axis passing through the centroid of cross-section BB (fig. 1). During the test, the total load  $P$  was

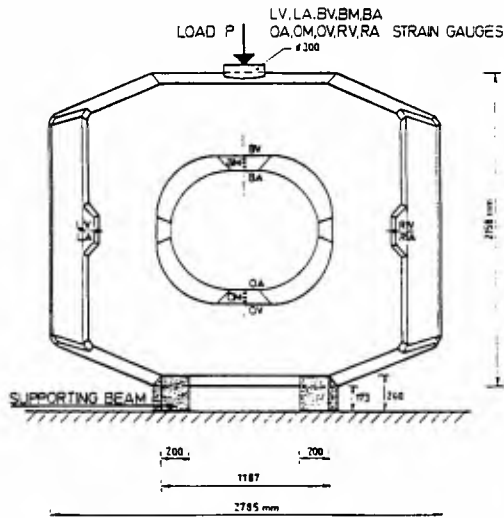


Figure 2. Test set-up for the static loading test

increased by increments of 200 kN. At each load level the deformation of the concrete surface was measured at 10 different points by means of strain gauges with a gauge length of 60 mm. The strain gauges were positioned parallel to the original upper and lower faces of the block. The shortening of the minor axis of the central hole was measured along three verticals.

Rupture of the block occurred at a load level of 2400 kN which corresponds to 16 times the weight of the block itself. Fig. 3 shows the HARO after failure.



Figure 3. Block after the static loading test

The shortening of the short central axis BM-OM in relation to the applied load  $P$  is shown in fig. 4. From this figure it appears that the elastic state extends to about 1600 kN. Beyond this value the shortening of the axis BM-OM increases at a higher rate. This non-linear behaviour is confirmed by the strain gauge readings. Measured strains and strains found in a supporting 3-dimensional linear elastic finite element analysis correspond reasonably well for loads up to  $P = 1600$  kN, as is shown in fig. 5 for strain gauge LA. From this load level on, the course of the measured strain signals varies rather widely depending on the location of the strain gauges. This is due to the fact that during the loading process the internal stress distribution gradually changes and that only local strains are measured. The maximum measured (tensile) strain equals  $190 \cdot 10^{-6}$  (strain gauge BV).

As the static loading test concerns, the total input energy is obtained as the surface under the load-displacement curve. Associating the decrease  $\Delta d$  of the axis BM-OM with the displacement at the point load, one can obtain from fig. 4 the energy values mentioned in table 1.

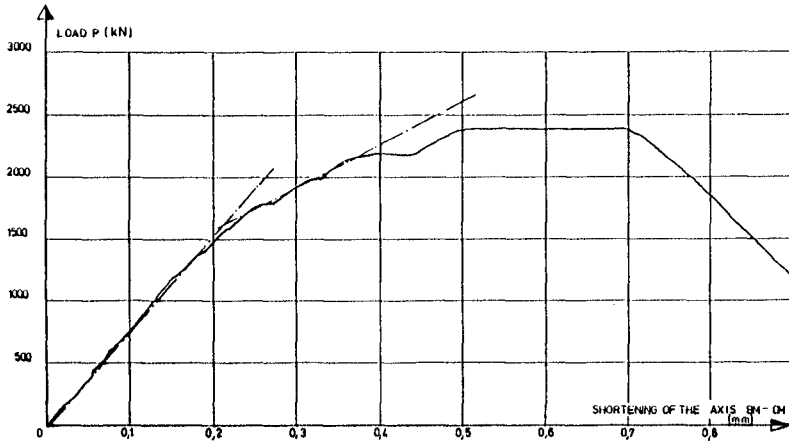


Figure 4. Shortening of the axis BM-OM as function of the load P

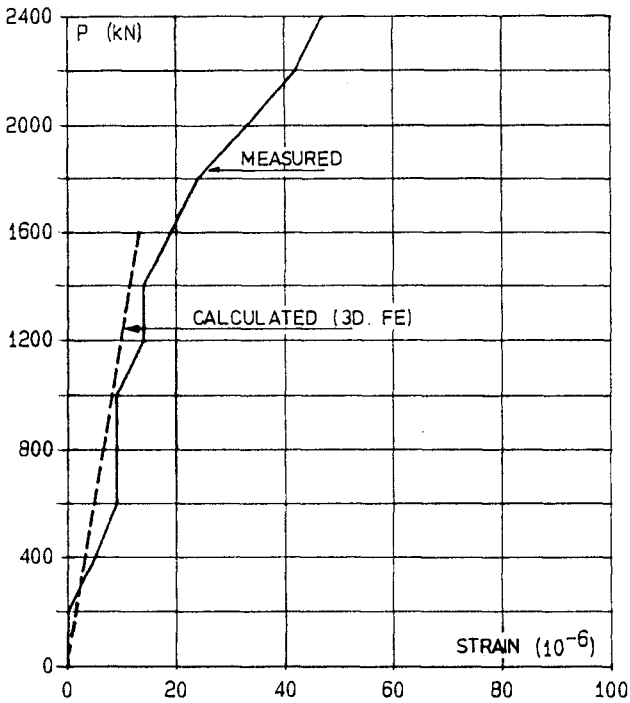


Figure 5. Comparison of measured and calculated strain at LA

**TABLE 1 - Static loading test**

P (kN)	$\Delta d$ (mm)	$E_i$ (kJ)
1600	0.21	0.252
2400	0.5	0.800
2400	0.7	1.280

After the test, cores were drilled at the upper and lower face of the block. On the cores (113 mm in diameter and 100 mm in height) compression and splitting tests were performed. Compressive strengths equal to 43.4 MPa and 48.7 MPa were found respectively for the upper and lower surface. Values of 3.08 MPa (upper surface) and 3.67 MPa (lower surface) were obtained for the splitting tensile strength. Each value represents the mean of three test results.

#### **4. DYNAMIC LOADING TEST IN THE LABORATORY**

The test set-up for the dynamic loading test is essentially the same as for the static one. The impact is performed by means of a falling steel block, having a mass of 516 kg. The vertical movement of the block is guided by two steel laths which fit, with some margin, in vertical notches at two opposite side faces of the steel block. The lifting hook is designed in such a way that delocking takes place almost instantaneously.

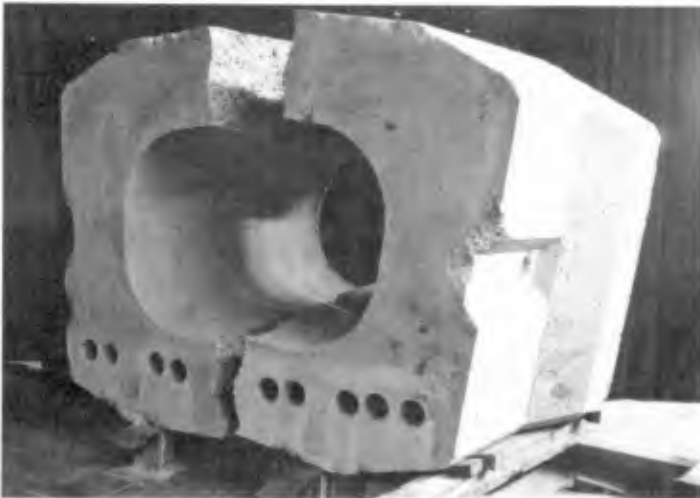


Figure 6. Block after the dynamic loading test

The height of fall, being equal to 50 mm the first time, was successively increased by 50 mm increments until complete failure of the HARO took place. The following cracking sequence could be observed by the naked eye :

- drop height of 650 mm : vertical crack at the upper inner face, extending to the front and back face.
- drop height of 700 mm : vertical crack at the lower inner face.
- drop height of 750 mm : horizontal crack at the left inner face.
- drop height of 800 mm : extension of the vertical cracks and rupture of the block into two parts (fig. 6).

In fig. 7, the maximum tensile strain, recorded during the impact at the locations RA, BM, LA and OM is plotted. It follows that after the impact from 550 mm height, cracking already occurred at the lower inner face (OM). The maximum strain at the upper inner face appears to remain almost constant at a value of 180 microstrain from the impact from 250 mm height on. Noteworthy is that the maximum concrete strain, again corresponds to the usual range i.e. 150-200  $10^{-6}$ , as encountered in the static loading test.

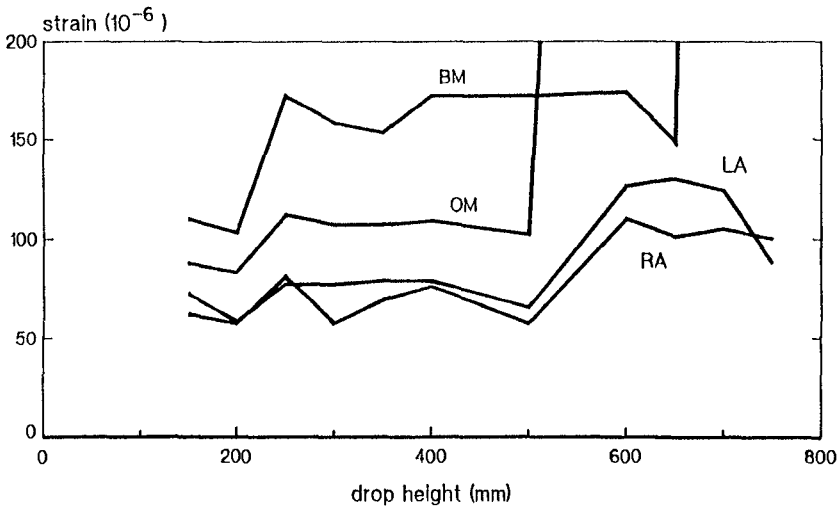


Figure 7. Measured peak strains during impact

The energy input corresponding to the potential energy of the impactor is obtained from

$$E_i = m_i g \Delta h \tag{1}$$

where  $m_i$  : mass of the impactor (516 kg)  
 $g$  : gravitational acceleration  
 $\Delta h$  : drop height.

For  $\Delta h$  equal to 550 mm (onset of damage) and 800 mm (complete rupture) the values  $E_i$ , mentioned in table 2, are obtained. As it was observed that rebound of the impactor

**TABLE 2 - Dynamic test in the laboratory**

$\Delta h$	$E_i$ (kJ)
550 mm	2.784
800 mm	4.050

remained very limited, these values can reasonably be considered as the energy absorbed by the HARO block. The values mentioned in table 1 are considerably smaller than those given in table 2.

From the dynamic measurements, the impact time was calculated as 0.7 ms.

## **5. PENDULUM TESTS ON THE SITE**

### **5.1. General description**

Armour units should be able to withstand impacts from adjacent units. These impacts can occur while placing the units on the slope or under wave attack. In order to simulate these impacts, pendulum tests were carried out on site.

A 150 kN HARO suspended by a cable at the top of a crane jib was first given a horizontal deviation  $d$  from its equilibrium position and then swung against other blocks at rest on a rock bed (fig. 8). Two different impact situations were envisaged (fig. 8). In the first test, the impact block hits two blocks of an adjacent row. In the second test, an edge of the impact block hits another block on its weakest side. The first situation results from the design placement pattern (a block of an upper row rests against two blocks of the lower row). The second is deemed to correspond to an exceptional event.

### **5.2. First test series**

The first series of tests is performed according to the first impact situation. The horizontal deviation  $d$  before release was progressively increased by 0.50 m. The final deviation amounted to 7.00 m. No further increment was possible due to technical limitations imposed by the crane. None of the blocks was broken. Only the three directly involved blocks were locally damaged at the protuberances.

In table 3, values of the maximum accelerations measured at different locations on the back side of the impact block are mentioned. No reliable strain measurements were obtained during the test series.



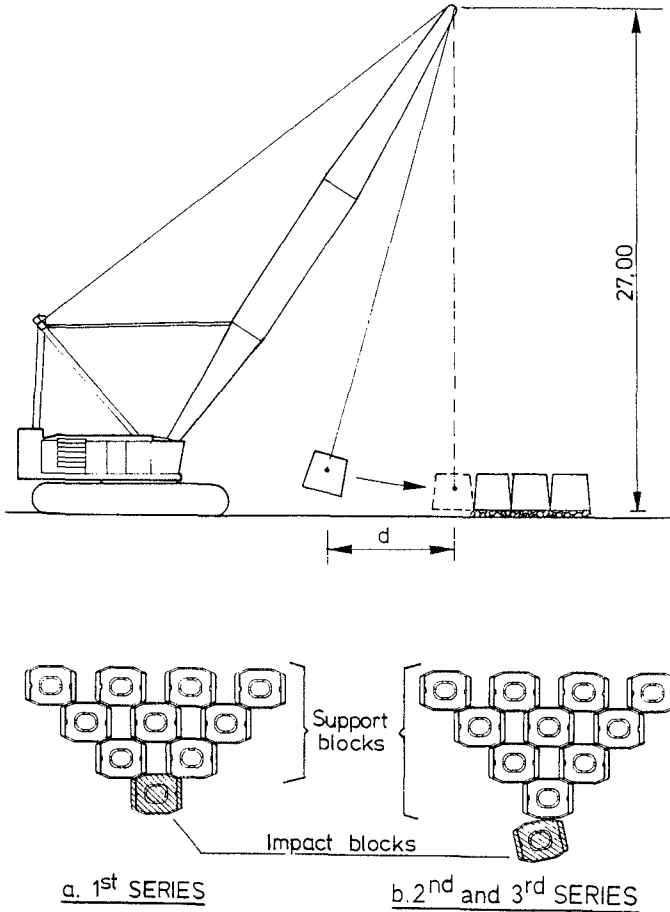


Figure 8. Test set-up for pendulum test on site

The input energy  $E_i$  corresponding to the potential energy of the impact block, calculated by (1) is also indicated in table 3. Also indicated is the value  $0.5 E_i$ , which will be useful for the evaluation of the second and third test series (see sections 5.3 and 5.4). The energy values mentioned in table 3 are considerably larger than those mentioned in tables 1 and 2. However, the impact phenomenon is quite different and obviously the bending stresses are much lower for this first site configuration.

**5.3. Second test series**

The second series of tests was performed according to the second impact situation envisaged in 5.1. This situation is rather similar to the dynamic loading test performed in the Laboratory (section 4).

**TABLE 3 - First test series : accelerations and potential energies  $E_i$** 

Horizontal deviation d (m)	$\Delta h$ (m)	Accelerations ( $m/s^2$ )				$E_i$ (kJ)	$0.5 E_i$ (kJ)
		A1	A2	A3	Mean		
3.0	0.174	510	220	180	300	25.6	12.8
4.0	0.310	530	340	400	400	45.6	22.8
4.5	0.392	110	30	20	50	57.7	28.8
5.0	0.485	620	270	360	420	71.4	35.7
5.5	0.588	420	370	300	360	86.5	43.3
6.0	0.702	280	200	310	260	103.2	51.6
6.5	0.826	830	1010	750	860	121.5	60.8
7.0	0.960	1000	1020	780	930	141.2	70.6

The deviation was progressively increased by steps of 1 m. The target block showed severe transverse cracks after the impact out from the 4 m deviation. In table 4, peak values of accelerations and strains are mentioned. The locations of the accelerometers A and the strain gauges R are as follows :

- A1 and A2 : back side of target block (opposite to the impact face)
- A3 : front side of impact block (opposite to the impact face)
- R1 : inner back face of target block
- R2 : inner side face of target block
- R3 : inner front face of target block
- R5 : inner back face of impact block
- R6 : inner side face of impact block.

**TABLE 4 - Second test series**

Deviation d (m)	Peak accelerations ( $m/s^2$ )			Peak strains ( $10^{-6}$ ) (↗ indicates strain gauge failure)				
	A1	A2	A3	R1	R2	R3	R5	R6
1	200	190	210	9	2	3	-	-
2	360	220	140	140	6	14	50	-
3	450	880	330	160	10	25	12	2
4	730	1590	850	↗	41	↗	8	16

The maximum peak strain, before rupture of strain gauge R1, is equal to  $160 \cdot 10^{-6}$  which indicates that for the three tests considered so far, the maximum concrete strain could be considered as a useful failure criterion. In fig. 9, the recorded strain signal from strain gauge R3 is shown for the impact from  $d = 3$  m. It follows that the impact time is about 12 ms. Fig. 10 shows the acceleration signal A3 for the same impact situation. The second impact at about 295 msec is caused by the rotation of the impact block after the first contact at one of the edges. It has to be noted that the time scales of figs. 9 and 10 are different.

Only in a very limited zone of the front face of the target block, local crushing of the concrete occurred during the first few impacts. This indicates that the energy release in the contact zone remained small. This locally damaged zone had a diameter of about 0.25 m and was located at a height of about 0.50 m.

**5.4. Third test series**

The third test series was also performed according to the second impact situation. The target block was replaced by a new one but the impact block was the same as in the second test series. Only deviations equal to 1 and 4 m were realized. At the latter impact, severe transverse cracks occurred this time in the impact block. Measured peak accelerations of the impact block are given in table 5.

**TABLE 5 - Third test series : accelerations (m/s<sup>2</sup>)**

Deviation d (m)	A1	A2	A3
1	90	20	60
4	720	1350	410

**5.5. General remarks**

- The results of the tests according to the first impact situation, which could occur during regular placing of the blocks, indicate that under these circumstances no rupture of the blocks seems possible in practice.
- The second, accidental impact situation, appears to be more critical. Comparison of the second and third test series indicates that the stress fields generated both in the impact and the target block, cause damage of comparable magnitude. Hence the mention of  $0.5 E_j$  in table 3.
- The input energy at  $\Delta h = 800$  mm in the laboratory test equals 4.05 kJ whereas at  $d = 4$  m, a value of 22.8 kJ is obtained for the pendulum test. A comparison only based on energy values, appears not to be appropriate.
- Interpretation of the dynamic behaviour on the basis of the acceleration measurements

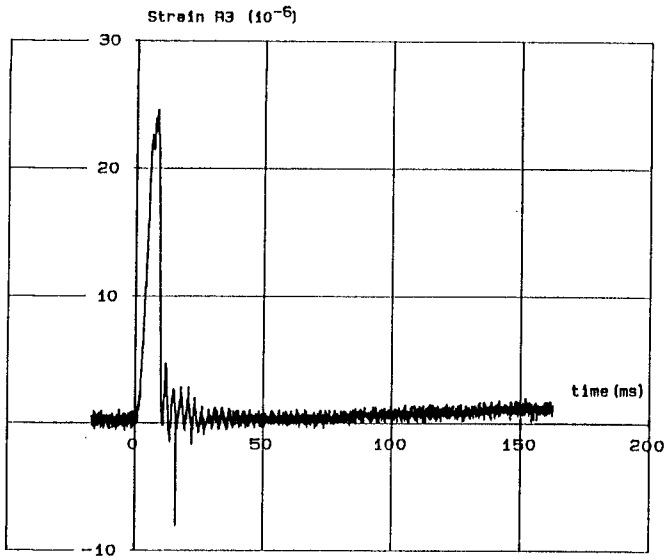


Figure 9. Strain signal R3 during impact from  $d = 3$  m (second test series)

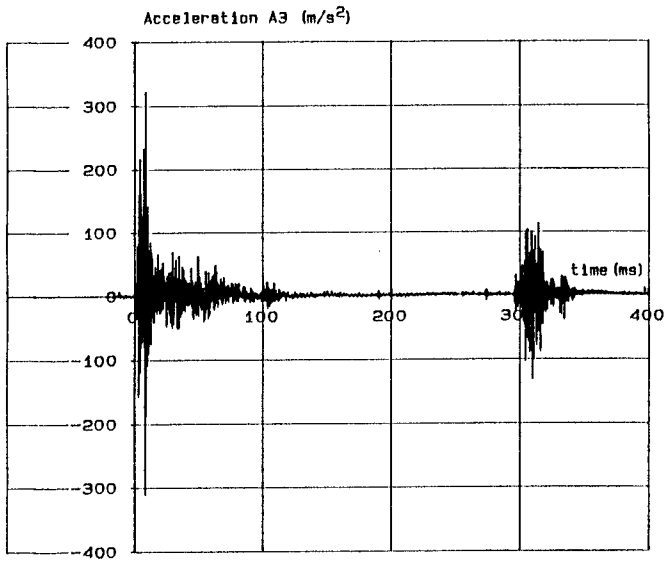


Figure 10. Acceleration signal A3 during impact from  $d = 3$  m (second test series)

is not straightforward. Regarding the first impact situation, contact with the two adjacent blocks at rest never occurs simultaneously and hence the energy distribution between the different blocks turns out to be quite complex. In the second impact situation considered, the impact block starts to rotate during the edge contact. This results in a contribution of rotations to the measured total acceleration signal which cannot be separated from the acceleration due to the main pendulum movement.

## **6. FURTHER CONSIDERATIONS WITH REGARD TO STRENGTH**

For plain concrete armour units, structural integrity depends to a large extent on the absence of significant cracks, and thus on the concrete tensile strength. A major problem in this respect is cracking due to thermal stresses caused by the hydration process. Temperature measurements in both grooved cubes and HAROs were carried out during the first days after casting (Van Damme et al., 1988). Due to the central opening in the HARO the temperature increase remained small and resulted in a considerable reduction of the thermal stresses at early age. No thermal cracks are observed in the approximately 11000 HARO units manufactured in Zeebrugge.

## **7. CONCLUSIONS**

- During a static loading test in the laboratory, the HARO block failed at a load of 2400 kN, which represents 16 times its own weight.
- During a dynamic loading test in the laboratory, rupture of a block took place after the impact of a steel block with a mass of 516 kg from a drop height of 800 mm.
- Pendulum tests on the site were performed according to two different configurations (lower part of figure 8). When the impact block was swung in between two other blocks, up from a horizontal deviation of 7 m, only local damage of the blocks occurred. When the impact block hit an adjacent block at its weakest side, failure of the blocks occurred for a horizontal deviation of 4 m.
- Although the general structural shape of the HARO is less robust than a massive cube, the results of static and dynamic loading tests on a 150 kN block confirm the adequate structural performance. Indeed, the tests prove that during regular placing of the individual armour elements no rupture of the blocks seems possible in practice. Even in case of an accident, e.g. dropping of a block during placement, the chance for damage of the blocks remains negligible.
- From a structural point of view the maximum concrete strain can be considered as a useful failure criterion both in static and dynamic loading conditions. Further research on concrete to concrete impact with large-scale tests would provide a better understanding of the failure mechanism.
- It can be stated that all investigations (hydraulic stability, run up, structural strength, durability), the experience on site (fabrication and placement on the slope) and the favourable cost price show that the HARO perfectly fulfils all performance criteria required for armour units.

## **8. ACKNOWLEDGMENT**

The authors gratefully acknowledge the assistance of J. Vyncke (formerly with the Magnel Laboratory, now with the Scientific and Technical Centre for the Building Industry at Brussels) during the dynamic test in the laboratory.

## **9. REFERENCES**

1. De Rouck J., Wens F., Van Damme L., Lemmers J. : Investigations into the merits of the HARO-breakwater armour unit,  
Proc. 2nd COPEDEC, Beijing 1987, Vol. II. pp. 1054-1068.
2. Van Damme L., Taerwe L., Dedeyne R., De Rouck J. : Quality and durability of concrete armour units,  
Proc. XXIst I.C.C.E., Torremolinos - Malaga, Spain 1988.  
Vol. 3. Ch. 156, p. 2102-2115.
3. Wens F., De Rouck J., Van Damme L. : Comparative laboratory investigations on HARO, grooved cubes, dolos and tetrapods,  
(to be published in "Coastal Engineering", Delft).